Research Article | Vol. 32, No. 4 / 12 Feb 2024 / Optics Express 6154

Optics EXPRESS

# Multiconfiguration afocal freeform telescopes

AARON BAUER,* CHI ZHANG, YUXUAN LIU, AND JANNICK P. ROLLAND

*The Institute of Optics, University of Rochester, 480 Intercampus Drive, Rochester, NY 14627, USA*
*aaron.bauer@rochester.edu*

**Abstract:** An approach to designing multiconfiguration afocal telescopes is developed and demonstrated. Freeform surfaces are used to maximize the achievable diffraction-limited zoom ratio while staying in a compact volume for a two-position multiconfiguration afocal optical system. The limitations of these systems with three-mirror beam paths are discussed and subsequently overcome by introducing an additional degree of freedom. In a four-mirror beam path system, the goal of a 5x zoom ratio is achieved with a compensated exit pupil and diffraction-limited performance. A significant benefit in optical performance when using freeform surfaces is shown compared to more conventional surface types.



## 1. Introduction

As applications for imaging systems become more diverse, the required optical specifications of the systems become increasingly complex and challenging to achieve with a single fixed-focus imager. Optical designers must scour their toolboxes for all available tools to meet the requirements of the next generation of systems. Using all-reflective optics, which are intrinsically achromatic, enables a single system to be used for multiple spectral bands with the additional benefit that mirrors are more amenable to large aperture sizes than lenses. All-reflective systems can be unobscured to maximize the light throughput for a given aperture size. When freeform optics [1] are applied to unobscured reflective telescopes, they have been shown to provide substantial reductions in the root-mean-square (RMS) wavefront error (WFE) and system volume [2–4], as well as to provide additional flexibility for other more system specific requirements [5–8].

Additional system flexibility can be achieved by utilizing an afocal system. Afocal foreoptics allow for the largest optics of a system to be untethered to a specific format sensor, providing the system with spectral and application flexibility [9–13]. By combining the technology of freeform optics with an afocal architecture, a highly adaptable and highly performant system can be designed. Bauer *et al.* found significant benefit is provided to unobscured, reflective afocal systems by adding freeform optics, including improving the quality of the exit pupil [4], which is necessary for a seamless integration with other imaging optics.

Operational flexibility for an optical system can be taken one step further by using a zoom system offering continuous imaging over the zoom range or by a multiconfiguration system, where a finite number of optical configurations are utilized. The most common type of zoom or multiconfiguration system is one where the focal length or magnification can be varied between a high and a low value. This feature allows a scene to be surveyed (low magnification) or inspected (high magnification), thus providing flexibility to be used in various situations. Using reflective optics in a zoom system offers similar benefits as in fixed focus optics and, though not common, is present in the literature as focal imaging systems using off-axis conic surfaces [14] or freeform surfaces [15–17] and as an afocal imaging system using off-axis conic surfaces [12].

This work will combine freeform optics with an afocal two-position multiconfiguration system to create a novel optical system with the ultimate flexibility. Compared to a continuous zoom system, a two-position multiconfiguration system maintains the full benefit imaging at the extrema

#516961 https://doi.org/10.1364/OE.516961
Journal © 2024 Received 26 Dec 2023; revised 25 Jan 2024; accepted 26 Jan 2024; published 6 Feb 2024

Optics EXPRESS

configurations (high- and low-magnification) but does not need to expend design degrees-of-freedom on the in-between magnifications, thus decreasing the system complexity for a given zoom ratio. In this paper, we explore the design possibilities within the space of three-mirror and four-mirror systems, including the achievable optical performance, zoom ratio, and system volume, using a novel method to create the afocal magnification changes. We also demonstrate the significant advantage that freeform optics have in this space compared to designs using more conventional off-axis conic surfaces.

## 2. Motivation for the design specifications

While the multiconfiguration method to be introduced in Section 3 can be applied generally to a variety of optical systems and applications, to best demonstrate the concepts and to make the optical design specifications used for the design studies in this work realistic and relevant, we hypothesized an application for the optical systems. To assist in the surveyance and examination of the impact of natural disasters, a satellite in low-earth orbit will house the to-be-designed two-position multiconfiguration afocal telescope. It boasts a wide-field, low-magnification configuration for general scene observation and a narrow-field, high-magnification configuration for targeted search activities. In the high-magnification configuration, a 250 mm entrance pupil diameter and a 1° x 1° full field-of-view (FOV) give a 1.9 m resolution and a 12 km x 12 km imaging area on the ground. To match the afocal optics to an imager with a 25 mm entrance pupil, the high-magnification configuration must have an afocal magnification of 10x. We are targeting a 2x afocal magnification in the low-magnification configuration, which gives a 5x zoom ratio. The full FOV of the low-magnification configuration is 5° x 5° with an entrance pupil diameter of 50 mm. On the ground, this translates to imaging a 60 km x 60 km imaging area with a 9.4 m resolution. These parameters are illustrated in Fig. 1. We are aiming for a maximum mirror size of ~250 mm, which corresponds to a typical maximum fabrication capacity of our manufacturing partners. With a 250 mm entrance pupil diameter specification in the high-magnification configuration, the low-magnification configuration must be constrained to use a sub-aperture of the primary mirror within the same 250 mm.

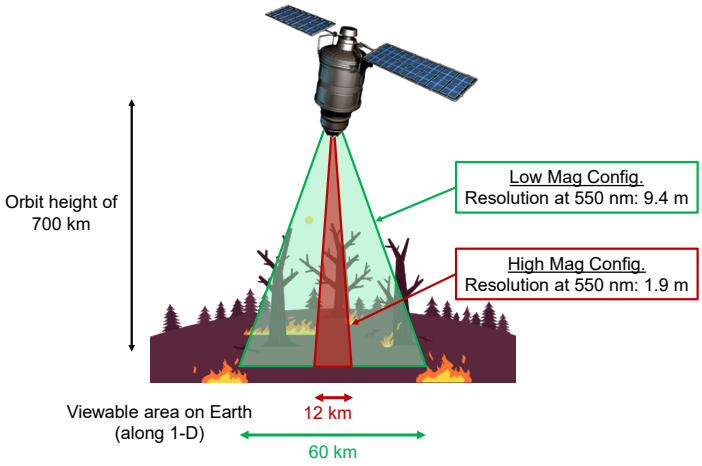


**Fig. 1.** An illustration of the natural disaster observing application that motivated the design specifications.

Optics EXPRESS

## 3. Method used for first-order optical property variation

When designing a multiconfiguration optical system, the mechanisms for changing the first-order optical properties of the system are less constricted compared to a continuous zoom system. A continuous zoom system must have some variable(s) that are smoothly and continuously varied to provide continuous first-order property changes (i.e., the translation of optical elements). A multiconfiguration system is not restricted to only continuous variable changes and can even have different beam paths for each configuration. Further, a continuous zoom system must have every motion coordinated with all other motions such that the correct combination of positions is present at all times. A two-position zoom system only requires precision at the motion endpoints for the moving components. The path that the optics take from one endpoint to the other is not important, nor is the coordination between the motions. When the optics arrive in the vicinity of the endpoint, a kinematic mount can provide a precision location and orientation when a switchable load is applied to hold it in place, such as from a magnet.

For the two-position multiconfiguration designs in this work, we implement a method that results in two separate (yet similar) beam paths. To describe this method, we will assume that each configuration has a three-mirror beam path, meaning that the light in each configuration interacts with three mirrors. The three mirrors in each path may or may not be the same three mirrors. In the two configurations, the primary mirror (M1) is shared and has two tilt positions about its local X-axis, allowing the reflected light to be incident on one of two separate secondary mirrors (M2a, M2b). The light for both configurations uses the primary mirror over the same aperture as was described as design requirement in Section 2 and thus, the two differentiated tilt states of the primary mirror are required to eliminate surface-ray obscurations. The separated secondary mirrors (M2a, M2b) can have completely different surface shapes and locations in space. Following a reflection from each respective secondary mirror, the light from both paths is incident on a shared tertiary mirror (M3) that can translate and tilt in space when switching between the two configurations. Additionally, the object-space aperture stop is allowed to translate in the Y-direction. This two-position multiconfiguration method using a three-mirror beam path is illustrated in Fig. 2 (with an uncompensated exit pupil location), for which the design results are formally presented in Section 5.3.

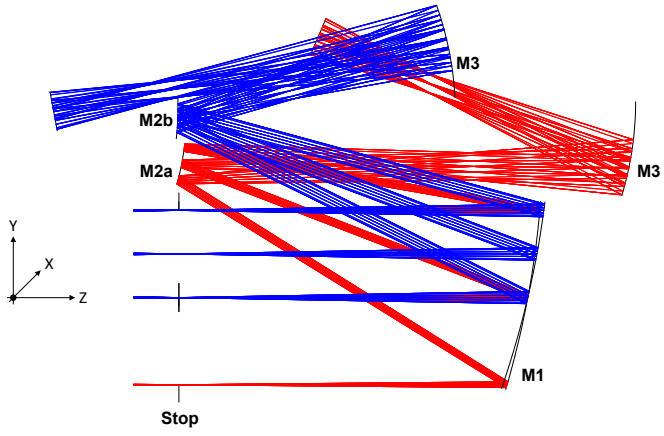


**Fig. 2.** Concept layout of a three-mirror beam path optical system using a novel approach to a multiconfiguration system where M1 can tilt to direct light to separate M2 mirrors (M2a or M2b), after which the light interacts with a shared M3 that can translate and tilt in space. In this illustration, the exit pupil locations are uncompensated. The red rays are for the high-magnification configuration, and the blue rays are for the low-magnification configuration.

Optics EXPRESS

We explored a variation of the three-mirror beam path system described above where the tertiary mirror is also separated (M3a, M3b) to provide an additional degree of freedom in Section 5.5. The same zoom motion concept can be applied to systems with beam paths of more than three mirrors, where each additional mirror could be separated or shared. To demonstrate the design advantages of using an additional mirror, we explored the space of a four-mirror beam path with a shared primary mirror, a separated secondary mirror, a shared tertiary mirror, and a shared quaternary mirror in Section 6.2. Finally, we separated the tertiary mirror in the four-mirror beam path designs and evaluated the improvements to the optical performance in Section 6.3. For convenience, the motions of the optics in each design group in the subsequent Sections are shown in Table 1. As will be seen in the design results, by utilizing separate beam paths and surface tilt changes between configurations in addition to the more traditional zoom motions of surface translations, an impressive combination of wavefront performance, compactness, and zoom ratio can be achieved. A comparison to traditional zoom motion systems is presented in Section 6.4.

**Table 1. Motion of the optics for each group of designs in the subsequent sections. α-tilt is a rotation around the local X-axis of the component. Refer to Fig. 2 for the coordinate axes**

| System Group | M1 | M2 | M3 | M4 |
|---|---|---|---|---|
| Section 5.3–5.4 | α-tilt | Separated, fixed | α-tilt, Y-Z translation | N/A |
| Section 5.5 | α-tilt | Separated, fixed | Separated, fixed | N/A |
| Section 6.2, 6.4 | α-tilt | Separated, fixed | α-tilt, Y-Z translation | α-tilt, Y-Z translation |
| Section 6.3 | α-tilt | Separated, fixed | Separated, fixed | α-tilt, Y-Z translation |

## 4. Exit pupil parameters in multiconfiguration afocal systems

The concept motivating using an afocal system as foreoptics is to mate it to an existing imaging system that focuses the collimated light exiting the afocal foreoptics to a sensor. To combine the two subsystems most optimally, the entrance pupil of the existing image system must be matched in size, location, and angle to the exit pupil of the afocal system. Thus, it is vital to maintain a solid understanding of the exit pupil properties of the afocal system to facilitate its use with an existing imaging system. Beyond the first-order properties of the exit pupil (location, size, and tilt), there are higher-order effects known as pupil aberrations that impact the overall quality of the exit pupil and can have detrimental effects on the pupil-matching condition [18–21]. The quantification of the pupil aberrations is beyond the scope of this work. Instead, our goal is to quantify the general pupil quality and improve it through the optimization processes introduced by Bauer et al., where there was a demonstrated trade-off in optical performance when implementing exit pupil quality constraints [4]. Two types of pupil error are described – RMS pupil size error and RMS pupil offset error. The pupil size error looks at the size and shape of the real exit pupil for each field point and compares it to the perfect exit pupil size and shape. Pupil size error is synonymous with distortion for an afocal system (i.e., change in afocal magnification with field). By directly controlling the real exit pupil size error to within a required amount, the distortion of the system is controlled to within the same requirement. In this work, we aim for an RMS exit pupil size error (distortion) of $< 5\%$, which is typical of freeform telescopes. The pupil offset error quantifies the difference in the axial location of the real exit pupil relative to the defined exit pupil plane. Errors in the pupil offset manifest as a mismatch between the exit pupil of the afocal telescope and entrance pupil of the existing imaging system for which the afocal telescope serves as foreoptics. That mismatch translates to vignetting (loss of light), so aiming for an RMS pupil offset error of $< 5\%$ is a reasonable goal.

The ideas of a compensated or uncompensated multiconfiguration system are also relevant for the systems designed in this work, so it is leveraged to explain the concepts. In a focal zoom

Optics EXPRESS

or multiconfiguration system where the light is focused on a detector, a change of one group of powered optical elements (such as a translation) changes the focal length of the system. However, it also has the effect of changing the back focal distance of the system. So, while a single change in the configuration can yield the required focal length variation, the image will not be in focus for a stationary sensor plane. This scenario is referred to as an uncompensated zoom system. The sensor must be moved throughout the zoom motion to ensure an in-focus image. While doable, it is not ideal from a system-level standpoint. The preferred option is to move another group of powered optics coordinated with the first group's motion to give the desired focal length change and keep the image in focus at a stationary sensor plane. This situation is referred to as a compensated system. In general, $N$ first-order optical properties that change through zoom (e.g., focal length and back focal distance) requires $N$ first-order changes in the optical layout to satisfy.

While the description of compensated and uncompensated multiconfiguration systems was given for focal systems, the same concepts apply for afocal systems. For an afocal system, the focal length is replaced by the afocal magnification and the back focal distance is replaced by the location of the exit pupil. In the case of an afocal system, having a compensated exit pupil is even more attractive since an uncompensated zoom would require coordinating the motion of an existing imaging system through zoom to ensure that it correctly matches up to the moving exit pupil of the afocal system.

## 5. Three-mirror design space

### 5.1. First-order optical property considerations

Before designing a two-position multiconfiguration system with three-mirror beam paths, we must first understand what is feasible. The most critical aspect to study is the number of required first-order constraints compared to the number of changeable first-order variables between the two configurations. The afocal magnification change is the first and most apparent first-order constraint between the two configurations. The second first-order constraint is the location of the two exit pupils in space, where a compensated system would require the two exit pupils to be coincident. The third constraint affected by the choice of the first-order mirror powers is the Petzval curvature.

The variables that affect the first-order optical properties between zooms, illustrated in Fig. 3, are the curvatures of the separate M2s, the M1-M2 airspace, the M2-M3 airspace, and the location of the aperture stop in object space. However, the M1-M2 airspace and the aperture stop have limited movement possible due to ray clearance requirements for the former and ray clearance and packaging requirements for the latter. Thus, these two variables can help refine the first-order specifications but are not completely free variables.

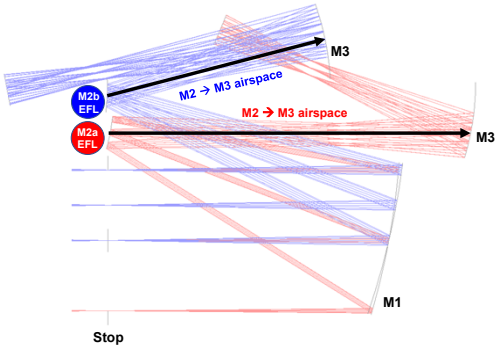


**Fig. 3.** Illustration of the free variables that impact the first-order optical properties between configurations.

Optics EXPRESS

In summary, for a three-mirror beam path system, there are three first-order constraints to hold between the configurations but only two free variables with which to hold those constraints. Holding the afocal magnification constraint is non-negotiable, and it is necessary to balance the Petzval curvature using negative and positive mirrors if there is to be any hope of achieving a diffraction-limited design [4,22]. Thus, the location of the exit pupil is unconstrained, meaning for a three-mirror beam path system using the described method for switching between configurations, only uncompensated multiconfiguration systems are feasible to design with high performance. If a system is desired that is less mechanically complex with fewer moving parts and, thus, fewer first-order design variables, there must be a tradeoff with achievable first-order constraints, such as Petzval curvature (imaging performance).

### 5.2. Design methods and constraints

In our prior work, we designed numerous fixed magnification freeform afocal systems that meet the specifications for the high-magnification configuration of this system [4]. We started with one of the designs that could be corrected to much better than the diffraction limit using only low-order Zernike terms (up to Z10 in Fringe ordering), indicating that the design form was well-behaved and could be easily altered without sacrificing performance. We also chose a system whose volume (70 L) was large enough to accommodate a second configuration without causing obscuration challenges. The selected starting design is shown in Fig. 4.

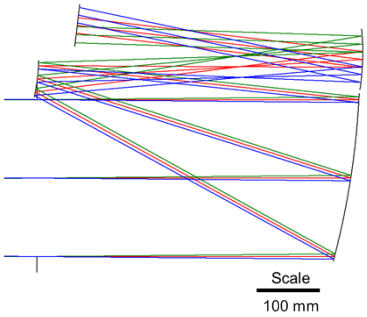


**Fig. 4.** Starting 10x afocal magnification design for the multiconfiguration system. This design meets the specifications of the high-magnification configurations and is corrected below the diffraction limit at a volume of 70 L.

The first step to increasing the zoom ratio is to give the fixed magnification starting design a second but identical configuration. As the optimization progresses, the afocal magnification of the second configuration is slowly decreased from 10x via optimization constraints. As the afocal magnification is decreased, the entrance pupil diameter must also decrease to maintain a constant exit pupil diameter. Similarly, the FOV must be increased as the afocal magnification is reduced to maintain a constant angle of light at the exit pupil. The zoomed parameters are the field points, the decenter and diameter of the aperture stop, the tilt of M1, the M1-M2 airspace, the surface shape and tilt of M2, the M2-M3 airspace, and M3's Y-decenter and α-tilt (rotation about the local X-axis).

Our preferred method of design optimization for freeform systems, both afocal and focal, has been well-established at this point [22,23] and, thus, is not the focus of this paper. However, it is instructive to list the constraints we used during the optimization due to their importance in determining the results. We implemented the afocal magnification constraint as described in [4]. When a surface is shared between the two configurations, we allow that surface to decenter to allow for the used area to shift, providing more independent aberration correction. However, the amount of decenter must be limited to ensure that the shared surface does not grow too large.

Optics EXPRESS

In these studies, we limited the decenter to 45 mm. As is typical for off-axis geometries, we implemented clearance constraints for each configuration and between configurations, which is essential when using separate M2s or different sections of shared mirrors. Finally, we found that the volume of the system preferred to increase indefinitely, so a volume constraint was applied to keep the system size reasonable. The final design specifications are shown in Table 2. While following the freeform aberration correction principles of [22], the afocal magnification of the second configuration was continually decreased from 10x until no further zoom ratio increase was possible while meeting the performance requirements. All optimizations and analyses were performed using an angular-based image space with a planar reference wavefront. During the design phase, we investigated two additional optimization methods. The first alternate method consisted of identical starting configurations at a midpoint afocal magnification, then increasing the afocal magnification of one configuration while decreasing the afocal magnification of the other configuration. The second alternate method explored starting with two configurations that were optimized independently to give a desired zoom ratio from the start, then optimized together to converge on a solution. Neither of these latter two methods produced results better than the chosen method as described above. The design method is summarized in a flowchart in Fig. 5.

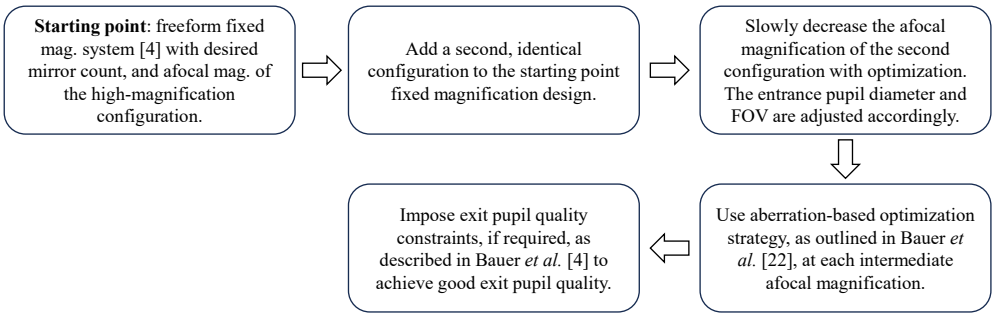


**Fig. 5.** Flowchart summary of the design method for the two-position zoom systems.

**Table 2. Design specifications for the three-mirror beam path systems**

| Parameter | Units | High Magnification | Low Magnification |
|---|---|---|---|
| Afocal magnification | - | 10x | 2x (goal) |
| Entrance pupil diameter | mm | 250 | 50 (goal) |
| Full field-of-view | deg | $1 \times 1$ | $5 \times 5$ (goal) |
| Exit pupil diameter | mm | 25 | |
| RMS WFE ($\lambda$=587 nm) | waves | $< 0.07$ | |
| Volume | L | Minimize | |
| RMS pupil offset error | % | $< 5$ | |
| RMS pupil size error | % | $< 5$ | |
| Zoom ratio | - | 5 (goal) | |

### 5.3. Design results

After implementing the design methods as described above, we were able to successfully arrive at two-position zoom systems at a 2x and 3x zoom ratio, as shown in Fig. 6. Each design is diffraction-limited at $\lambda = 587$ nm and, as described in Section 5.1, is limited to have uncompensated exit pupils that require motion of the existing imaging system to stay aligned with the exit pupil

Optics EXPRESS

if it is be used as foreoptics. A 3x zoom ratio is the maximum diffraction-limited zoom ratio that could be achieved without encountering major pupil quality issues. These systems were first optimized without constraints on pupil quality while minimizing the package size. The 2x zoom ratio system met the pupil quality requirements without implementing constraints, but the pupil quality of the 3x system quickly degraded. To remedy this shortcoming, exit pupil quality constraints were implemented to improve the exit pupil [4]. However, instead of trading-off wavefront performance for a better pupil, we opted to illustrate a different type of trade-off. We increased the allowed decenter on the shared mirror (M3) from 45 mm to 60 mm, which subsequently required a larger volume system (75 L → 100 L). We also added more freeform terms (up to 14th order in FRINGE Zernike) to the shared mirror (M3), where the off-axis usage makes higher-order terms that typically provide negligible value useful. By allowing these design changes, we could control the exit pupil quality to nearly within specification (6% pupil offset in the high-magnification configuration).

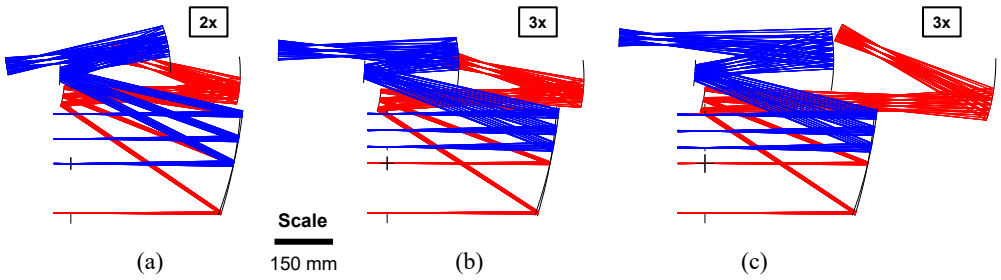


**Fig. 6.** 2D layouts of uncompensated diffraction-limited three-mirror beam path designs for zoom ratios of (a) 2x and (b) 3x. By increasing the volume and shared mirror decenter and using high-order freeform terms to describe the shared surfaces, the pupil quality of the 3x zoom ratio design in (b) was improved to meet the specification, resulting in (c). The volumes of the respective designs are (a) 60 L, (b) 75 L, and (c) 100 L.

### *5.4. Comparison to off-axis conic designs*

Comparing a freeform design to an off-axis conic design is a classic exercise highlighting the advantages of freeform optics. Off-axis conic optics have the potential to be easier to manufacture and measure (using nulling interferometry [24,25]), so there must be a convincing reason to transition to freeform surfaces. To highlight the benefits of freeform surfaces for this class of two-position multiconfiguration afocal telescopes, we completed an off-axis conic design with the exact specifications of the 2x zoom ratio system from the previous section. The resulting off-axis conic design is shown in Fig. 7, together with the corresponding freeform design. The freeform design achieved an RMS WFE approximately 2.7x better than the off-axis conic design when averaged over the two configurations. That degree of improvement is significantly greater than is typically seen for fixed focus or fixed magnification designs, often in the 1.5x improvement range. To understand the results, we fit the surface shapes in the freeform design with off-axis conics and looked at the magnitude of the residual departure, as listed in Table 3. For M1 and M2 (both), the departure from an off-axis conic is not substantial, but the shared M3 substantially departs from an off-axis conic. This data highlights the importance of using freeform surfaces to describe the shared surfaces because they allow greater control across the full aperture of the surface where each configuration uses overlapping sub-apertures.

Optics EXPRESS

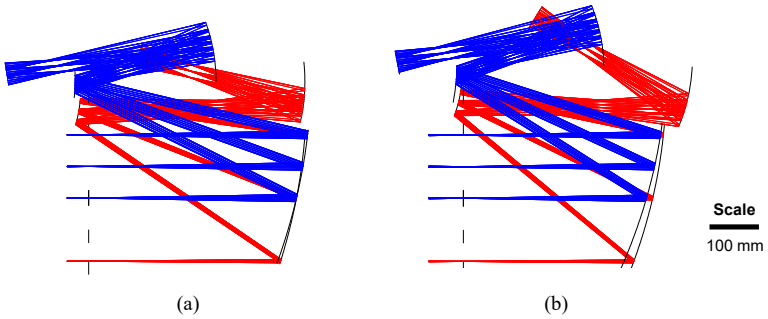


**Fig. 7.** 2D layouts of uncompensated three-mirror beam path designs with a zoom ratio of 2x for (a) freeform surface shapes and (b) off-axis conic surface shapes. The maximum RMS WFE over the full FOV for the freeform design is 0.068λ (high mag) and 0.065λ (low mag). The maximum RMS WFE of the off-axis conic design over the full FOV is 0.15λ (high mag) and 0.21λ (low mag), with λ=587 nm.

**Table 3. Residual departures of the 2x zoom ratio freeform mirrors after fitting with an off-axis conic surface**

| Mirror | Departure from off-axis conic (Peak-to-Valley) [μm] |
|---|---|
| Primary (M1) | 2.1 |
| Secondary (M2a) | 3.4 |
| Secondary (M2b) | 5.5 |
| Tertiary (M3) | 200 |

### *5.5. Variation on the three-mirror beam path to enable compensated exit pupils*

As stated in Section 5.1, with a three-mirror beam path system, three first-order constraints must be held to get a high-performing and compensated design, yet there are only two free first-order variables. The lack of variables limits a three-mirror beam path system using this multiconfiguration method to an uncompensated system, which is unsuitable for most applications. Another first-order variable that can change between configurations must be added to achieve a compensated design. A four-mirror beam path accomplishes that task and will be explored in Section 6, but we can still achieve a compensated system with a three-mirror beam path by altering the multiconfiguration method. Instead of a shared M3, it is split into two mirrors, similar to M2. The separate M3 mirrors would have independent shapes and locations and would be stationary through zoom, meaning the only optic motion required to switch the configuration is the M1 tilt. One caveat is that the separate M3 mirrors cannot both lie on the same centerline with the exit pupil, so only the location of the exit pupil is the same between the configurations. The exit pupil tilt (i.e., the direction of the outgoing on-axis chief ray) varies slightly between the configurations. However, by putting a fold mirror at the location of the exit pupil whose tilt can be coordinated with the tilt of M1, any imaging subsystem used with this afocal system can remain stationary when switching between the configurations as the fold mirror would properly direct the light. For this method, designs with 2x, 3x, and 4x zoom ratios are shown in Fig. 8. Each design is diffraction-limited and meets the exit pupil quality requirements. In this study, using high-order freeform terms did not appreciably help with performance or pupil quality, which can be attributed to the lack of off-axis shared mirrors. Thus, the only additional parameter to leverage for improved performance is the system volume, which is evident moving from the 3x

Optics EXPRESS

to the 4x design (75 L to 115 L). Zoom ratios greater than 4x are not included as they require unrealistic volumes to meet the design goals.

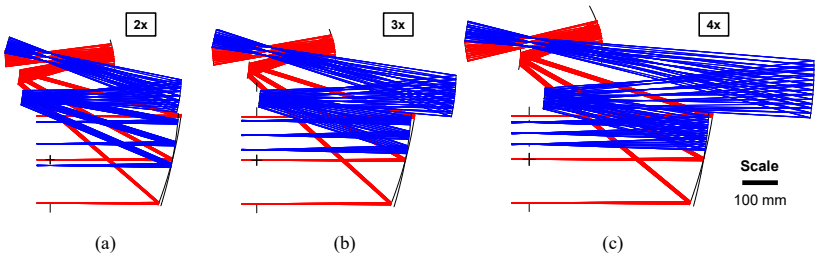


**Fig. 8.** 2D layouts for the systems using a separate secondary and tertiary mirrors. Diffraction-limited performance was achieved for zoom ratios of (a) 2x, (b) 3x, and (c) 4x while meeting the exit pupil quality requirements. The volumes of the systems are 55 L, 75 L, and 115 L for the 2x, 3x, and 4x zoom ratios, respectively.

## 6. Four-mirror beam path designs with compensated exit pupils

It was shown in Section 5.1 that the original three-mirror beam path designs did not have enough degrees of freedom that affected the first-order properties between the configurations to allow for the exit pupils to be constrained to be coincident while simultaneously achieving good wavefront performance. In Section 5.5, another degree of freedom was added that allowed good wavefront performance and coincident exit pupils, but the tilt of the exit pupil was not the same between the configurations, and the size of the systems was large. A method to address both shortcomings of the three-mirror beam path variation is to introduce a fourth freeform mirror into the beam path. Specifically, the designs described in this section share a single large primary mirror, use a separated secondary mirror, and share a single tertiary and quaternary mirror. The motion of the primary mirror is limited to tilts about its vertex, but the tertiary and quaternary mirrors can translate in Y and Z and rotate about X when switching the configurations.

### *6.1. Finding a good starting point*

Multiple methods were investigated to find the optimal starting point. Our initial two paths tried to leverage the multiconfiguration designs we had already completed. We first tried simply adding a fourth mirror to the already optimized three-mirror beam path designs from Section 5.3 and slowly moving the exit pupils closer together using design constraints. That method was unsuccessful as the inertia was too high to push the design out of the three-mirror beam path solution space. We next tried returning to the three-mirror fixed magnification starting point and adding a fourth mirror, then constraining the exit pupils to remain coincident as the zoom ratio increased. This method was mildly successful but still resulted in large-volume systems. The method that produced the best designs was to create a new four-mirror beam path starting design from scratch. Each mirror could then be fully leveraged, and the design would not be stuck in a three-mirror beam path solution space. The four-mirror beam path starting design is shown in Fig. 9.

### *6.2. Four-mirror beam path optimization and designs*

From this starting point, we used the same optimization strategy described in Section 5.2. We started with identical configurations with 10x afocal magnification. We then methodically worked the afocal magnification of the second configuration down as far as it would go while meeting the design specifications. When a certain zoom ratio was reached, we would then focus on reducing

Optics EXPRESS

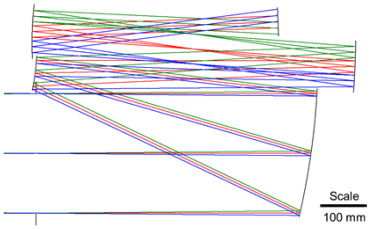


**Fig. 9.** Starting point for the four-mirror beam path designs. Both configurations begin in identical 10x afocal magnification layouts.

the volume of the system at that zoom ratio. The resulting designs are shown in Fig. 10. We achieved more compact volumes compared to any of the designs in prior Sections. For the 2x and 3x zoom ratios, diffraction-limited performance was achieved, and the pupil quality metrics were satisfied at a volume of 35 L. At a 4x zoom ratio, the pupil quality metrics were becoming more challenging to maintain, so we allowed this design to have a larger offset of 75 mm between the center of the rays for each configuration on M3 and M4. This change resulted in a system with a slightly larger volume. Even with this change, however, the pupil offset error was limiting, so we allowed it to be a somewhat larger 7%. Wavefront performance was not a limiting factor as we pushed the design to a 5x zoom ratio, which was the project's ultimate goal. However, as with the 4x zoom ratio, pupil quality becomes the limiting factor, measuring 10% for both offset and size error. These designs leverage the benefits of using higher-order terms (up to 14$^{th}$-order Zernikes) on the shared mirrors to maximize performance while minimizing volume and exit pupil errors.

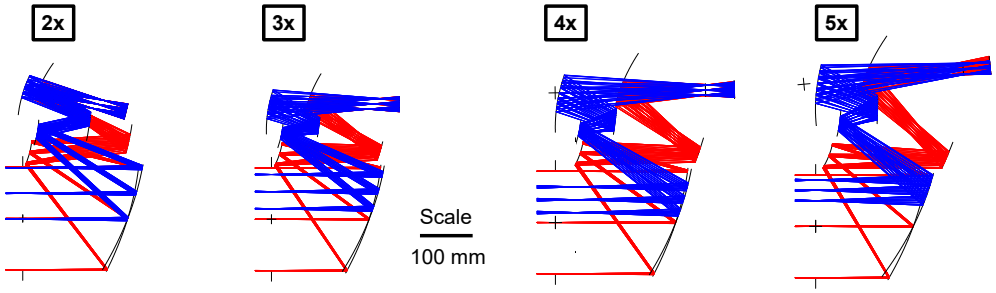


| Parameter | 2x | 3x | 4x | 5x |
|---|---|---|---|---|
| Volume | 35 L | 35 L | 50 L | 50 L |
| RMS pupil size error | < 4% | < 5% | < 5% | < 10% |
| RMS pupil offset error | < 2% | < 5% | < 7% | < 10% |
| M3/M4 Decenter | 45 mm | 45 mm | 75 mm | 75 mm |

**Fig. 10.** Design results for the four-mirror beam path systems.

### *6.3. Four-mirror beam path variation for better exit pupil quality*

If an application requires a 4x or 5x zoom ratio with better exit pupil quality than the designs in Fig. 10, we can modify the arrangement just like we did for the three-mirror beam path designs. By changing the tertiary mirror from a shared mirror to two separate mirrors, we can improve the quality of the exit pupil for the 4x and 5x zoom ratios to < 5% RMS while maintaining a compact volume (50 L) and diffraction-limited performance. The four-mirror beam path with variation designs are shown in Fig. 11.

Optics EXPRESS

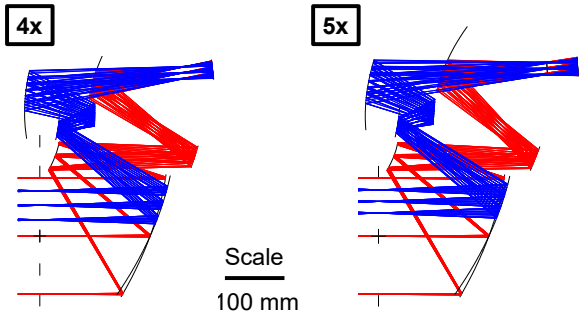


**Fig. 11.** 4x and 5x zoom ratio designs using the four-mirror beam path variation. The volume of each system is 50 L.

### 6.4. *Comparison to OAC systems and traditional zoom motion systems*

For the four-mirror beam path designs, we expected that the OAC designs would not be able to achieve the same levels of performance as the freeform designs, especially for small volumes. Thus, we chose to compare the freeform design to OAC designs at two different volumes – 50 and 100 L. Furthermore, OAC designs struggle to get beyond a 2x zoom ratio, so the zoom ratio was fixed at 2x to maintain a fair comparison. The results are shown in Fig. 12. The freeform surfaces excel at the 50 L volume, providing 12x better RMS wavefront error and roughly 2x better exit pupil quality, while at the 100 L volume, the OAC designs put up a better fight, though were still outmatched by 4.5x in wavefront and roughly 2x in exit pupil quality. Like in our earlier OAC comparison, we attribute the magnitude of improvement going from OACs to freeform to the ability to better describe the ideal surface shapes for the shared mirrors that have separated used apertures between the two configurations.

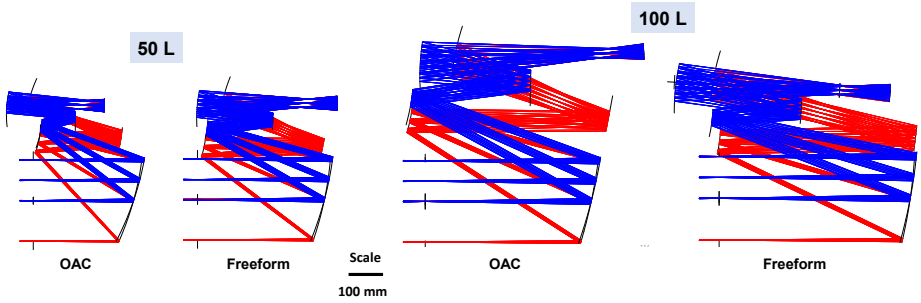


| Volume | 50 L | 50 L | 100 L | 100 L |
|---|---|---|---|---|
| Surface type | OAC | Freeform | OAC | Freeform |
| RMS pupil size error | < 8% | < 4% | < 7% | < 3% |
| RMS pupil offset error | < 7% | < 5% | < 8% | < 3% |
| RMS WFE (λ = 587 nm) | High Mag: 0.27λ<br>Low Mag: 0.37λ | High Mag: 0.026λ<br>Low Mag: 0.024λ | High Mag: 0.049λ<br>Low Mag: 0.058λ | High Mag: 0.012λ<br>Low Mag: 0.012λ |

**Fig. 12.** 2x zoom ratio OAC and freeform design comparison at 50 L and 100 L volumes with a four-mirror beam path.

Finally, it is instructive to compare the zoom motion concept introduced in this work to systems utilizing more traditional zoom motion. For the context of this comparison, a system with traditional zoom motion is one that uses all shared mirrors and mirror translation as the sole motion type to create the afocal magnification change. We designed a freeform traditional zoom

Optics EXPRESS

motion system with a two-position, 2x zoom and the same specifications as the 100 L freeform design shown in Fig. 12 with the goal of minimizing the wavefront error in tandem with exit pupil size and offset errors. The comparison is shown in Fig. 13. The traditional zoom motion system is outperformed in wavefront by 4x and 9x in the high- and low-magnification configurations, respectively. Further, the exit pupil offset error is 2x better in the low-magnification configuration for the zoom method proposed in this work. This comparison illustrates the significant value of this new zoom method.

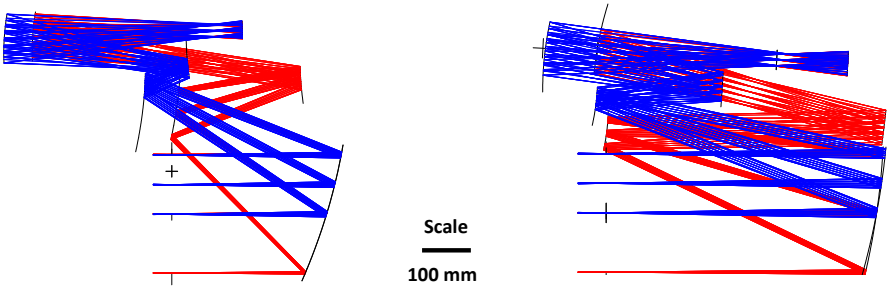


| Traditional | Zoom Type | Proposed |
|---|---|---|
| 100 L | **Volume** | 100 L |
| Freeform | **Surface type** | Freeform |
| High Mag: 2%<br>Low: Mag: 2% | **RMS pupil size error** | High Mag: 3%<br>Low Mag: 3.5% |
| High Mag: 3.5%<br>Low: Mag: 6% | **RMS pupil offset error** | High Mag: 2%<br>Low Mag: 3% |
| High Mag: 0.05λ<br>Low Mag: 0.11λ | **RMS WFE<br>(λ = 587 nm)** | High Mag: 0.012λ<br>Low Mag: 0.012λ |

**Fig. 13.** A comparison of two methods for achieving a discrete 2x, two-position zoom system. A traditional zoom motion method design (top, left) versus a design using the new method proposed in this work (top, right).

## 7. Conclusion

In this work, we conceived a method for designing a multiconfiguration optical system and showed the substantial impact that using freeform optics provides. To demonstrate the design method, multiple variations of a multiconfiguration afocal telescope were designed. We first discussed and showed the ability to achieve a two-position zoom using a three-mirror beam path, albeit with an uncompensated exit pupil. Then, by allowing the tertiary mirror to be split into two separate mirrors, we showed diffraction-limited designs up to a 4x zoom ratio with a compensated exit pupil. Adding a fourth mirror to the beam path allowed for a fully compensated system to be significantly minimized in size. Finally, splitting the tertiary mirror into separate mirrors in the four-mirror beam path design allowed further improvement of the exit pupil quality while maintaining a compact volume and diffraction-limited performance.

While this work was related strictly to demonstrating the possibilities for the optical design and a design-for-manufacture study is beyond its scope, any system to be built must be mechanically feasible. To that end, having a multiconfiguration system with a small volume, like the four-mirror beam path systems, serves a dual purpose. The first and most apparent is that the system is smaller, weighs less, and requires smaller optical surfaces. The less obvious benefit is that the moving optics have less distance to travel when switching between configurations. Care was taken in these designs to ensure no collision points between the optics when they move. By

Optics EXPRESS

utilizing these methods described herein, optical systems for applications requiring multiple imaging modalities can be designed with the ultimate flexibility in their use.

**Funding.** National Science Foundation (EEC-2310640, EEC-2310681, IIP-1822026, IIP-1822049).

**Acknowledgments.** This research was supported by the National Science Foundation I/UCRC Center for Freeform Optics (IIP-1822049 and IIP-1822026, EEC-2310640, EEC-2310681) and its industry members.

**Disclosures.** The authors declare that there are no conflicts of interest to this article.

**Data Availability.** Data underlying the results presented in this paper are not publicly available at this time but may be obtained from the authors upon reasonable request.

## References

1. J. P. Rolland, M. A. Davies, T. J. Suleski, *et al.*, "Freeform optics for imaging," Optica **8**(2), 161–176 (2021).
2. J. Reimers, A. Bauer, K. P. Thompson, *et al.*, "Freeform spectrometer enabling increased compactness," Light Sci Appl. **6**(7), e17026 (2017).
3. E. M. Schiesser, A. Bauer, and J. P. Rolland, "Effect of freeform surfaces on the volume and performance of unobscured three mirror imagers in comparison with off-axis rotationally symmetric polynomials," Opt. Express **27**(15), 21750–21765 (2019).
4. A. Bauer, C. Zhang, and J. P. Rolland, "Exit pupil quality analysis and optimization in freeform afocal telescope systems," Opt. Express **31**(15), 24691–24701 (2023).
5. T. Kampe, I. Franka, P. Spuhler, *et al.*, "Development and test of 3-mirror freeform telescope for Earth remote sensing applications," Proc. SPIE 12232 (2022).
6. Z. Tang and H. Gross, "Improved correction by freeform surfaces in prism spectrometer concepts," Appl. Opt. **60**(2), 333–341 (2021).
7. C. Yoon, A. Bauer, D. Xu, *et al.*, "Absolute linear-in-k spectrometer designs enabled by freeform optics," Opt. Express **27**(24), 34593–34602 (2019).
8. C. Liu, C. Straif, T. Flügel-Paul, *et al.*, "Comparison of hyperspectral imaging spectrometer designs and the improvement of system performance with freeform surfaces," Appl. Opt. **56**(24), 6894–6901 (2017).
9. T. Yang, J. Zhu, and G. Jin, "Starting configuration design method of freeform imaging and afocal systems with a real exit pupil," Appl. Opt. **55**(2), 345–353 (2016).
10. W. B. Wetherell, "AFOCAL SYSTEMS," in *Handbook of Optics: Volume I - Geometrical and Physical Optics, Polarized Light, Components and Instruments*, M. Bass, ed. (McGraw-Hill Education, 2010).
11. L. G. Cook, "Five-mirror afocal wide field of view optical system," U **054**(S10), 774 (2018).
12. R. S. Kebo, "All-reflective zoom optical system," US5 **144**, 476 (1992).
13. J. Johnson, C. Roll, A. Fontaine, *et al.*, "Wide field-of-view NURBS-based freeform afocal telescope," Proc. SPIE 12530 (2023).
14. R. B. Johnson, "Unobscured reflective zoom systems," Proc. SPIE 2539 (1995).
15. G. Xie, J. Chang, K. Zhang, *et al.*, "Off-axis three-mirror reflective zoom system based on freeform surface," Frontiers of Optoelectronics **9**(4), 609–615 (2016).
16. C. Xu, D. Cheng, J. Chen, *et al.*, "Design of all-reflective dual-channel foveated imaging systems based on freeform optics," Appl. Opt. **55**(9), 2353–2362 (2016).
17. L. Zettlitzer, H. Gross, S. Risse, *et al.*, "Reflective dual field-of-view optical system based on the Alvarez principle," Appl. Opt. **62**(31), 8390–8401 (2023).
18. J. Sasian, "Interpretation of pupil aberrations in imaging systems," Proc. SPIE 6342 (2006).
19. T. Smith, "The changes in aberrations when the object and stop are moved," Trans. Opt. Soc. **23**(5), 311–322 (1922).
20. C. G. Wynne, "Primary Aberrations and Conjugate Change," Proc. Phys. Soc. B **65**(6), 429–437 (1952).
21. J. Sasián, *Introduction to Aberrations in Optical Imaging Systems* (Cambridge University Press, 2013).
22. A. Bauer, E. M. Schiesser, and J. P. Rolland, "Starting geometry creation and design method for freeform optics," Nat. Commun. **9**(1), 1756 (2018).
23. K. Fuerschbach, J. P. Rolland, and K. P. Thompson, "Theory of aberration fields for general optical systems with freeform surfaces," Opt. Express **22**(22), 26585–26606 (2014).
24. T. J. Magner, J. Zaniewski, S. Rice, *et al.*, "Fabrication and testing of off-axis parabolic mirrors," Opt. Laser Technol. **19**(2), 91–96 (1987).
25. D. Malacara, *Optical Shop Testing* (John Wiley & Sons, 2007).